How Do Tropical, Northern Hemispheric, and Southern Hemispheric Volcanic Eruptions Affect ENSO Under Different Initial Ocean Conditions?

Article *in* Geophysical Research Letters · November 2018

DOI: 10.1029/2018GL080315

6 authors, including:

Fei Liu
Nanjing University of Information Science & Technology
47 PUBLICATIONS **563** CITATIONS
SEE PROFILE

Chen Xing
Nanjing University of Information Science & Technology
2 PUBLICATIONS **2** CITATIONS
SEE PROFILE

Deliang Chen
University of Gothenburg
355 PUBLICATIONS **9,631** CITATIONS
SEE PROFILE

Geophysical Research Letters

RESEARCH LETTER
10.1029/2018GL080315

Key Points:
- The IOC has a strong impact on the volcano-ENSO relationship only when it involves a strong El Niño
- A significant El Niño can be expected in the second/first winter after NH/tropical eruptions when the IOC is not a strong El Niño
- In the CESM simulation the volcanic cooling outweighs the Bjerknes feedback-induced warming

Correspondence to:
F. Liu,
liuf@nuist.edu.cn

Citation:
Liu, F., Xing, C., Sun, L., Wang, B., Chen, D., & Liu, J. (2018). How do tropical, Northern Hemispheric, and Southern Hemispheric volcanic eruptions affect ENSO under different initial ocean conditions? *Geophysical Research Letters*, *45*. https://doi.org/10.1029/2018GL080315

Received 29 MAY 2018
Accepted 4 NOV 2018
Accepted article online 9 NOV 2018

How Do Tropical, Northern Hemispheric, and Southern Hemispheric Volcanic Eruptions Affect ENSO Under Different Initial Ocean Conditions?

Fei Liu[1], Chen Xing[1], Liying Sun[1], Bin Wang[2], Deliang Chen[3], and Jian Liu[4,5,6]

[1]Earth System Modeling and Climate Dynamics Research Center, Nanjing University of Information Science and Technology, Nanjing, China, [2]Department of Atmospheric Sciences and Atmosphere-Ocean Research Center, University of Hawai'i at Mānoa, Honolulu, Hawaii, USA, [3]Department of Earth Sciences, University of Gothenburg, Gothenburg, Sweden, [4]Key Laboratory for Virtual Geographic Environment, Ministry of Education; Jiangsu Provincial State Key Laboratory Cultivation Base of Geographical Environment Evolution; School of Geography Science, Nanjing Normal University, Nanjing, China, [5]Jiangsu Provincial Key Laboratory for Numerical Simulation of Large Scale Complex Systems, School of Mathematical Science, Nanjing Normal University, Nanjing, China, [6]Jiangsu Center for Collaborative Innovation in Geographical Information Resource Development and Application, Nanjing, China

Abstract Current understanding of volcanic effects on El Niño–Southern Oscillation in terms of eruption type and initial ocean condition (IOC) remains elusive. We use last-millennium proxy reconstructions to show how volcanic impacts depend on eruption type and IOC. When the IOC is not a strong El Niño, it is likely that an El Niño will mature in the second winter following 79% ($p < 0.01$) of Northern Hemispheric eruptions and in the first winter following 81% ($p < 0.01$) of tropical and 69% of Southern Hemispheric eruptions. For a strong El Niño-IOC, no significant El Niño will occur in the first winter after any type of eruption. The eruptions need to be large enough to cause these diverse effects. Our last-millennium simulation confirms the IOC effect, except that a La Niña occurs in the first winter following most tropical eruptions due to overestimated volcanic cooling in the model.

Plain Language Summary Investigation of the volcanic effect on the El Niño–Southern Oscillation is important to understanding the climate variability excited by natural forcing. For the first time, we explore the combined effects of volcanic type and initial ocean condition, which have been found crucial to understanding the El Niño–Southern Oscillation evolution solely. Based on the reconstruction analysis in this work, we have enough confidence to predict an El Niño in the second winter following Northern Hemisphere eruptions and the first winter following tropical eruptions when the initial ocean condition does not involve a strong El Niño. Otherwise a La Niña should be predicted. This reconstruction analysis provides a good reference for the evaluation of models' performance with respect to the volcano-El Niño–Southern Oscillation relationship. The inconsistence of first-winter responses after tropical eruptions between the reconstructions and simulation found in this work calls for further investigation and model improvement. Our conclusions here are based on one model, but they may still provide some guidance to the Model Intercomparison Project on the climatic response to Volcanic forcing.

1. Introduction

The El Niño–Southern Oscillation (ENSO) is known as the most important interannual climate variability that has global impacts (Cai et al., 2015; Deser et al., 2010; McPhaden et al., 2006; Yeh et al., 2018). Volcanic eruptions are dominant external forcing that can excite interannual climate variability (Hegerl et al., 2003; Myhre et al., 2014; Robock, 2000; Schurer et al., 2014). Whether and how a volcanic eruption affects ENSO are important for understanding natural climate variability, attracting much research attention (Adams et al., 2003). Particularly, the likelihood of El Niño is found to increase after an explosive eruption during last millennium according to proxy-based reconstructions (Adams et al., 2003; D'Arrigo et al., 2009; Emile-Geay et al., 2008; Handler, 1984; Li et al., 2013; Liu et al., 2018; McGregor et al., 2010; Wilson et al., 2010). After tropical eruptions, global warming is observed with the El Niño-like sea surface temperature (SST) anomaly as the main cause of the warming (Lehner et al., 2016; Robock & Mao, 1992; Santer et al., 2014). However, many state-of-the-art models fail to simulate this El Niño-like response (Ding et al., 2014; Maher et al., 2015; McGregor & Timmermann, 2011; Wang et al., 2017).

To understand volcanic impacts on ENSO, some mechanisms based on model simulations are presented. For example, after a volcanic eruption, El Niño can be excited by tropical cooling through the dynamical thermostat mechanism (Maher et al., 2015; Mann et al., 2005; Ohba et al., 2013; Predybaylo et al., 2017), rapid surface cooling around the Maritime Continent (Ohba et al., 2013), suppressed tropical precipitation (Liu et al., 2018), and tropical African cooling-suppressed West African monsoon (Khodri et al., 2017). El Niño can also be excited by wind change associated with land-ocean temperature gradient (Predybaylo et al., 2017) and equatorward migration of the Intertropical Convergence Zone due to asymmetric hemispheric cooling (Liu et al., 2018; Pausata et al., 2015; Stevenson et al., 2016) or due to less evaporation in the subtropical cloudless region (Lim et al., 2016).

Different initial ocean conditions (IOCs) before the eruption are found to modulate the volcanic effects on ENSO. The simulated El Niño-like response after Northern Hemispheric (NH) eruptions is almost 3 times greater for a La Niña IOC or a neutral IOC compared to an El Niño IOC (Pausata et al., 2016). One year after a tropical eruption, a significant El Niño-like response is simulated except when the eruption occurs during a La Niña developing phase (Ohba et al., 2013; Predybaylo et al., 2017). These effects of IOCs are obtained from simulations only based on single type of eruption, and therefore remain elusive for other eruption types. Furthermore, such effects are not known in terms of long-term reconstructions.

Volcanic effects on ENSO depend on the type of eruption. Significant volcanic impacts on ENSO are found for large eruptions (Emile-Geay et al., 2008), and there is a threshold of volcanic strength above which the volcanic forcing can excite El Niño-like responses in ECHO-G model simulation (Lim et al., 2016). The latitude of eruption location also affects volcanic effects on ENSO. A reconstruction analysis reveals an El Niño event in the first winter following tropical eruptions and in the second winter following NH eruptions (Liu et al., 2018). This conclusion, however, is drawn without considering the IOC. In the models (Liu et al., 2018; Stevenson et al., 2016), an El Niño can be simulated in the second winter after NH eruptions, consistent with reconstruction analysis. In the first winter after tropical eruptions, however, only a La Niña-like cooling is be simulated, which is opposite to reconstructions. This strong surface volcanic cooling in the first winter after tropical eruptions is also simulated by Khodri et al. (2017). Volcanic effects on ENSO in terms of eruption type in reconstructions and simulations should therefore be considered together with IOCs.

As our current understanding of volcanic effects on ENSO remains elusive due to restricted reconstruction data, limited simulation sample size, and model fidelity, we will present new evidence on such volcanic effects using last-millennium reconstructions with a large set of major eruptions as well as a last-millennium model simulation.

2. Data and Method

In this work, an 1,100-year ENSO index from 901 AD to 2,000 AD is used, which is an average of 10 sets of normalized nine-year high-pass ENSO reconstructions for the boreal winter (Braganza et al., 2009; Cook et al., 2008; D'Arrigo et al., 2005; Emile-Geay et al., 2013; Li et al., 2011, 2013; Mann et al., 2000; McGregor et al., 2010; Stahle et al., 1998; Wilson et al., 2010). This averaged ENSO index is highly correlated (0.87; $p << 0.01$) with the October–March Niño3 index (averaged over 150°–90°W, 5°S–5°N) using the Hadley Centre Ice and SST version 1 for the period of 1871–2000 (Rayner et al., 2003). Details of this 1,100-year ENSO index can be found in Liu et al. (2018).

A millennium simulation of 1,500 years from 501 AD to 2,000 AD is performed to simulate volcanic effects on ENSO (Liu et al., 2018). The Community Earth System Model version 1.0 (CESM1) is used because of its good performance in simulating ENSO seasonality, amplitude, frequency, and teleconnection (Bellenger et al., 2014). This 1,500-year simulation with a resolution of T31 is conducted using the reconstructed volcanic forcing from Gao et al. (2008), based on a 2,000-year control run similar to that in Rosenbloom et al. (2013). In the simulation, beside the Niño3 index, the thermocline tilt, denoted by 100-m ocean temperature difference between the equatorial eastern Pacific (150°–90°W, 5°S–5°N) and western Pacific (120°–150°E, 5°S–5°N), is also considered to represent ENSO dynamics. In the simulation, December–February average is used to represent the boreal winter.

IOC is defined by the Niño3 index or thermocline tilt in the latest winter before the eruption. An IOC is referred to as a strong El Niño IOC (SEI) when it is larger than 0.5 standard deviation; otherwise, it is not a

Table 1
Reconstructed and Simulated Count Fractions of Positive (>0) and Large (>0.25 Standard Deviation) Niño3 Index to Total Niño3 Index for Different Eruptions and Background (BG) When the IOC Is a Strong El Niño (SEI; >0.5 Standard Deviation) or Not a Strong El Niño (NEI; <0.5 Standard Deviation) for the First Winter (Year 0) and the Second Winter (Year 1) Following the Eruption

	Y0 (All Vol)		Y1 (All Vol)	
	Count Frac > 0	Count Frac > 0.25	Count Frac > 0	Count Frac > 0.25
Rec BG (NEI)	55% (425/766)	45% (346/766)	60% (458/766)	47% (361/766)
Rec NH Vol (NEI)	48% (20/42)	40% (17/42)	**79% (33/42)**	**67% (28/42)**
Rec Tro Vol (NEI)	**81% (25/31)**	**65% (20/31)**	58% (18/31)	39% (12/31)
Rec SH Vol (NEI)	69% (9/13)	54% (7/13)	54% (7/13)	46% (6/13)
Rec BG (SEI)	43% (145/334)	31% (104/334)	33% (111/334)	26% (88/334)
Rec NH Vol (SEI)	50% (12/24)	33% (8/24)	29% (7/24)	25% (6/24)
Rec Tro Vol (SEI)	**13% (1/8)**	**13% (1/8)**	**75% (6/8)**	**63% (5/8)**
Rec SH Vol (SEI)	**15% (2/13)**	**15% (2/13)**	31% (4/13)	15% (2/13)
Sim BG (NEI)	52% (564/1088)	38% (409/1088)	48% (526/1088)	35% (385/1088)
Sim NH Vol (NEI)	56% (10/18)	39% (7/18)	44% (8/18)	33% (6/18)
Sim Tro Vol (NEI)	**21% (4/19)**	**16% (3/19)**	**84% (16/19)**	37% (7/19)
Sim SH Vol (NEI)	48% (13/27)	37% (10/27)	59% (16/27)	41% (11/27)
Sim BG (SEI)	30% (121/409)	21% (87/409)	39% (159/409)	27% (111/409)
Sim NH Vol (SEI)	21% (3/14)	14% (2/14)	43% (6/14)	29% (4/14)
Sim Tro Vol (SEI)	17% (1/6)	**0% (0/6)**	33% (2/6)	33% (2/6)
Sim SH Vol (SEI)	17% (1/6)	**0% (0/6)**	**17% (1/6)**	17% (1/6)

Note. Significant ($p < 0.01$) count fractions are shown in bold.

strong El Niño IOC (NEI). In this work, the response is called an El Niño when the Niño3 index is positive. Other threshold defining the El Niño event, such as 0.25 standard deviation, is also used (Table 1), and similar results are obtained, unless mentioned otherwise.

To analyze the 1,100-year reconstructed ENSO index, the newest volcano reconstruction is used to identify different volcano types (Sigl et al., 2015). The NH, tropical, and Southern Hemispheric (SH) eruptions are classified based on sulfate deposition in the ice sheets in the two polar regions. The strength of each eruption is also recorded by global volcanic aerosol forcing. In the simulation, the volcanic forcing has different meridional distributions based on bipolar sulfate depositions (Gao et al., 2008). Following the definition in Liu et al. (2016, 2018), we define an eruption as an NH event if the volcanic aerosol burden is zero at 40°S, as a SH event if it is zero at 40°N, and as a tropical event if it is above zero at both 40°S and 40°N. Thus, these three types of eruptions have their aerosols centered in the NH, tropics, and SH, respectively.

The superposed epoch analysis (Haurwitz & Brier, 1981) is used to investigate volcanic effects on ENSO (Adams et al., 2003; Fischer et al., 2007; Liu et al., 2018). A 15-year window symmetrically spanning the eruption is used for the composite. Significance is calculated by the bootstrapped resampling method with 10,000 random draws from the data in the period studied (Adams et al., 2003). The simple count fraction, defined by the ratio of selected cases to total samples, is also used. The count fractions for El Niño and La Niña responses can be calculated by the ratios of positive and negative to total Niño3 index, respectively. The background count fraction is also calculated to represent the internal variability. For example, there are 766 winters following an NEI during the 1,100 years. Among these 766 winters there are 425 positive-Niño3 winters; thus, the background count fraction for the El Niño is 55% (425/766) for an NEI (Table 1). In this work, a high confidence level of 99% is used to identify the significance of count fractions for different eruptions, and these significant count fractions are much higher than the background. Confidence intervals are calculated by using repeated (n = 10,000) random draws. Each time we select pseudo-"eruptions," with same sample size as the studied eruptions, from the background randomly. Significance is then evaluated by comparing percentiles from the random draw to the count fraction of real eruptions.

3. Results

3.1. Volcanic Impacts on ENSO Based on Reconstructions

During the 1,100 years, there are 66 NH, 39 tropical, and 26 SH eruptions (Table 1). In the first winter following NH eruptions, there is no significant response (Figure 1a). In the second winter, however, there is an El Niño-

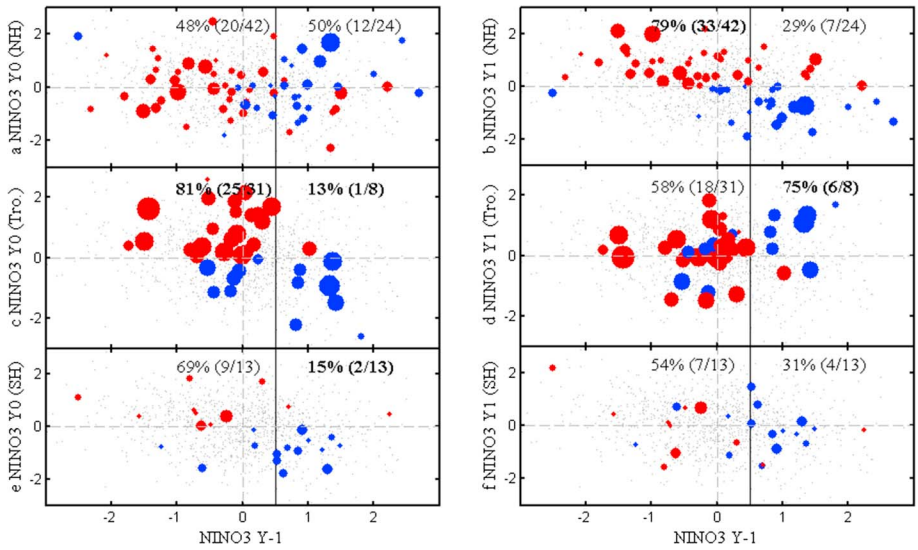

Figure 1. ENSO responses to different eruptions and IOCs in the 1,100-year (901–2000 AD) reconstructions. Reconstructed normalized Niño3 index in (a) first (year 0) and (b) second (year 1) winters following NH eruptions versus the initial Niño3 index in the winter (year −1) before eruptions. (c and d) Results for tropical eruptions and (e and f) for SH eruptions. The Niño3 index is normalized by its standard deviation. The logarithm of volcanic strength is proportional to the diameter of the color dot, with largest and smallest ones of 32.8 and 0.23 W/m^2, respectively. The red color denotes the Niño3 index above zero in year 1 for (a) and (b) and in year 0 for (c)–(f), and blue color denotes a negative value. The gray dot shows the result for each of the years during the 1,100-year period. The count fraction of positive to total index is also shown for IOC or Niño3 index at year −1 smaller or larger than 0.5, respectively. The significant ($p < 0.01$) count fraction is denoted by bold font.

like response for 79% (33/42; $p < 0.01$) of NH eruptions for an NEI (Figure 1b). This count fraction is much higher than the background of 60% (Table 1), meaning that the El Niño-like response is most likely excited by volcanic forcing rather than by internal variability. When the IOC involves a strong El Niño, the response may be El Niño- or La Niña-like. Without considering the IOC, the significance of the superposed epoch analysis on the ENSO response to NH eruptions is low (Liu et al., 2018).

A significant response to a tropical eruption mainly appears in the first winter following the eruption. There is a significant El Niño-like response in the first winter following 81% ($p < 0.01$) of tropical eruptions for an NEI (Figure 1c). For an SEI, the significant response is a La Niña-like cooling following 87% ($p < 0.01$) of the eruptions (Figure 1c). These two count fractions are much higher than the background ones of 55% and 57% (Table 1). A significant El Niño-like response is also found in the second winter for an SEI (Figure 1d). In the first winter after 85% ($p < 0.01$) of SH eruptions, there is a significant La Niña-like response for an SEI (Figure 1e). In this first winter, the El Niño-like response can be found after 69% of SH eruptions for an NEI.

When using 0.25 standard deviation as a threshold to define El Niño event, similar results are obtained. Although the count fractions for both background and responses are decreased, the count fractions for those significant responses remain much larger than those for the background (Table 1).

Some of these reconstructions give different results. In the reconstruction of Li et al. (2013), for example, the La Niña-like cooling is observed in the first winter following tropical eruptions, while the El Niño-like warming is observed in the second winter. Our conclusion based on the average of these 10 reconstructions is consistent with that based on instrumental observations. For the period of 1870–2010, El Niño-like warming also exists in the Hadley Centre Ice and SST version 1 in the first winter following the 1902 Santa Maria, 1963 Agung, 1982 El Chichón, and 1991 Pinatubo eruptions, but not following the 1883 Krakatau eruption (Khodri et al., 2017).

3.2. Volcanic Impacts on ENSO Based on Simulation

From 501 AD to 2,000 AD, there are 32 NH, 25 tropical, and 33 SH eruptions in the data set of Gao et al. (2008). For all these eruptions without considering their strength, significant El Niño responses only exist for tropical eruptions (Table 1). We further investigate volcanic effects for strong eruptions with the eruption-year aerosol

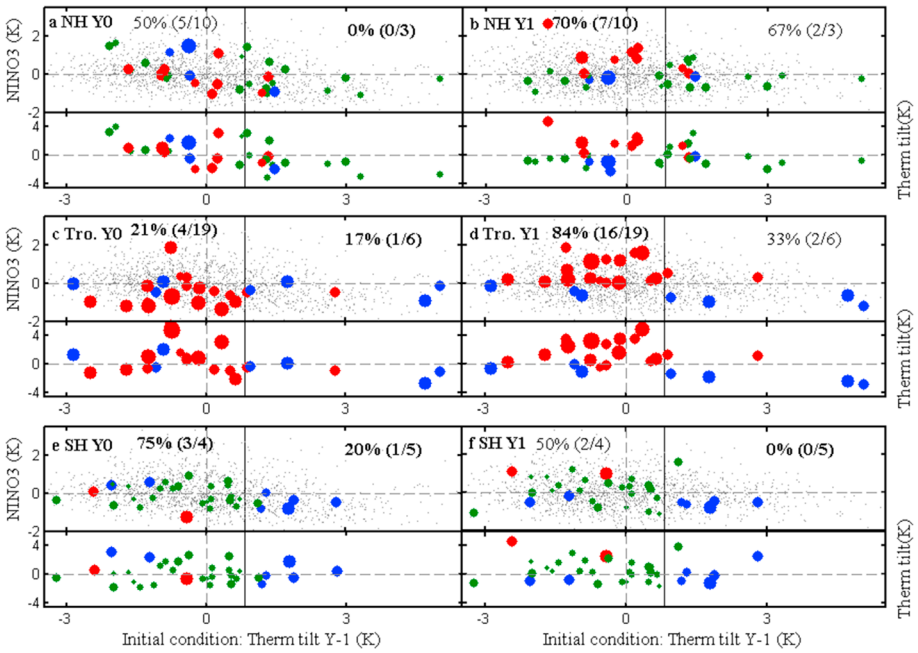

Figure 2. ENSO responses to different eruptions and IOCs in the 1,500-year (501–2000 AD) simulation. Niño3 index and thermocline tilt in (a) first (year 0) and (b) second winters (year 1) after NH eruptions versus initial thermocline tilt in the winter (year −1) before the eruption. (c and d) Results for tropical eruptions and (e and f) for SH eruptions. The logarithm of volcanic strength is proportional to the diameter of color dot. The red (blue) color denotes the Niño3 index above (below) zero in year 1 for large eruptions with aerosol concentration above 60 Tg at eruption year, and the results for small eruptions are shown by green dots. The gray dot shows the result for each of the simulated 1,500 years. The count fraction of positive to total index is shown for IOC or thermocline tilt at year −1 smaller or larger than 0.5 standard deviation or 0.8 K, respectively. The significant ($p < 0.01$) count fraction is denoted by bold font.

concentration above 60 Tg (Figure 2). For an SEI, no significant El Niño-like response can be identified in both first and second winters following NH eruptions (Figures 2a and 2b). Consistent with observations (Figure 1b), a significant El Niño-like warming is simulated in both SST and thermocline in the second winter for an NEI, and the count fraction reaches 70% ($p < 0.01$; Figure 2b), much higher than the background one of 48%.

In the first winter after 80% ($p < 0.01$) of large tropical eruptions, a significant La Niña-like response is simulated in SST regardless of IOC (Figure 2c). The simulated La Niña-like response for an SEI is consistent with the observation (Figure 1c). While when the IOC is not a strong El Niño, CESM1 still simulates a La Niña-like response in SST even some cases have El Niño-like responses in the thermocline, which is different from reconstruction analysis (Figure 1c). This La Niña-like response in the first winter is also found in the ensemble simulations of CESM (Stevenson et al., 2017). In the second winter following large tropical eruptions, both SST and thermocline exhibit consistent responses (Figure 2d). A significant El Niño-like response is simulated in SST following 84% ($p << 0.01$) of the eruptions for an NEI, which is much higher than the background of 48%.

When the IOC is not a strong El Niño, a significant El Niño-like response is simulated in the first winter after 75% ($p < 0.01$) of SH eruptions; otherwise, a significant La Niña-like response should be simulated in both first and second winters (Figures 2e and 2f).

When using 0.25 standard deviation as a threshold to define an El Niño event, similar results are obtained, except that the response in the second winter after tropical eruptions for an NEI becomes insignificant (Figure 2d). The reason is likely the overestimated volcanic cooling effect in CESM1.

3.3. Role of Volcanic Strength

In the reconstructions, the five significant resposnes, for example, El Niño responses in the second (first) winter after NH (tropical) eruptions (Figures 3a and 3b) for an NEI, La Niña response in the first winter after both tropical and SH eruptions for an SEI (Figure 3c), and El Niño responses in the second winter after tropical eruptions for an SEI (Figure 3d) and in the first winter after SH eruptions for a NEI (Figure 3e), exist for large

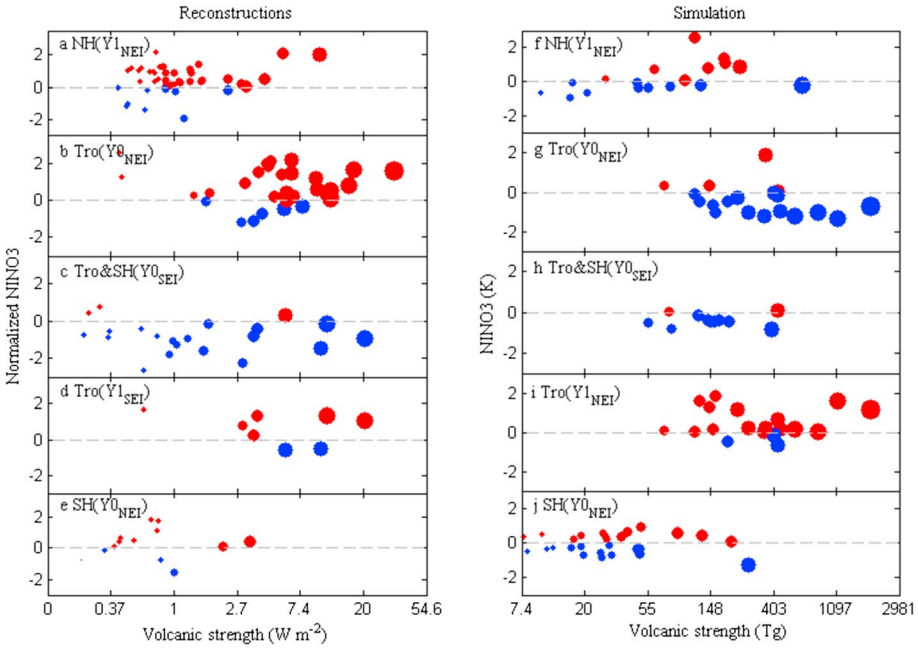

Figure 3. ENSO responses to volcanic strength in reconstructions and simulation. Niño3 index in the first (year 0) and second (year 1) winters as a function of logarithm of volcanic strength in (left) 1,100-year reconstructions and (right) 1,500-year simulation following different eruptions when the IOC is a strong El Niño (SEI) or not a strong El Niño (NEI). The logarithm of volcanic strength is proportional to the diameter of the dot. The red color denotes positive value, and blue, negative one.

volcanic eruptions when the forcing is larger than 0.37 W/m^2. The last two responses are not stable because of small sample size.

In the simulation, the significant El Niño responses in the second winter after NH eruptions (Figure 3f) and in the first winter after SH eruptions (Figure 3j) for an NEI exist only when the volcanic aerosol amount is larger than 60 Tg, although the latter is not stable. The significant La Niña response in the first winter after tropical eruptions for an NEI (Figure 3g), the El Niño response in the second winter after tropical eruptions for an NEI (Figure 3i), and the La Niña response in the first winter after both tropical and SH eruptions for an SEI (Figure 3h) all exist, and they are stable since the magnitude of these eruptions is large enough.

3.4. Possible Mechanisms

When the IOC does not involve a strong El Niño, warm SST anomaly occurs over the central equatorial Pacific in the first after NH eruptions (Figure 4a), accompanied by westerly wind anomaly over the western-to-central equatorial Pacific (Figure 4b). The reason is the equatorward migration of the Intertropical Convergence Zone due to interhemispheric thermal contrast of volcanic cooling (Liu et al., 2018; Pausata et al., 2015; Stevenson et al., 2016). The eastward gradient also appears in the thermocline for the first winter (Figure 4c). In the following year, the El Niño develops through the Bjerknes feedback.

In the first winter after strong tropical eruptions, eastward SST gradient (Figure 4d) and westerly wind anomaly (Figure 4e) appear over the equatorial Pacific. This is due to the dynamical thermostat mechanism associated with basin cooling (Maher et al., 2015; Mann et al., 2005; Ohba et al., 2013; Predybaylo et al., 2017), suppressed tropical precipitation (Liu et al., 2018), and rapid surface cooling around the Maritime Continent (Ohba et al., 2013). The suppressed African monsoon, shown in Khodri et al. (2017), can also be simulated (not shown), which is similar to Figure 7b of Liu et al. (2018). The El Niño-like response is also simulated in the thermocline (Figure 4f). The strong basin cooling over the equatorial Pacific, however, suppresses the eastward SST gradient-induced warming, resulting in SST cooling over eastern equatorial Pacific (Figure 4d). These divergent responses indicate that volcanic cooling may have been overestimated, and that the volcanic cooling effect is much larger than the volcano-excited Bjerknes feedback in CESM1. In the second winter, the stratospheric volcanic aerosol concentration decays quickly (Gao et al., 2008; Liu et al.,

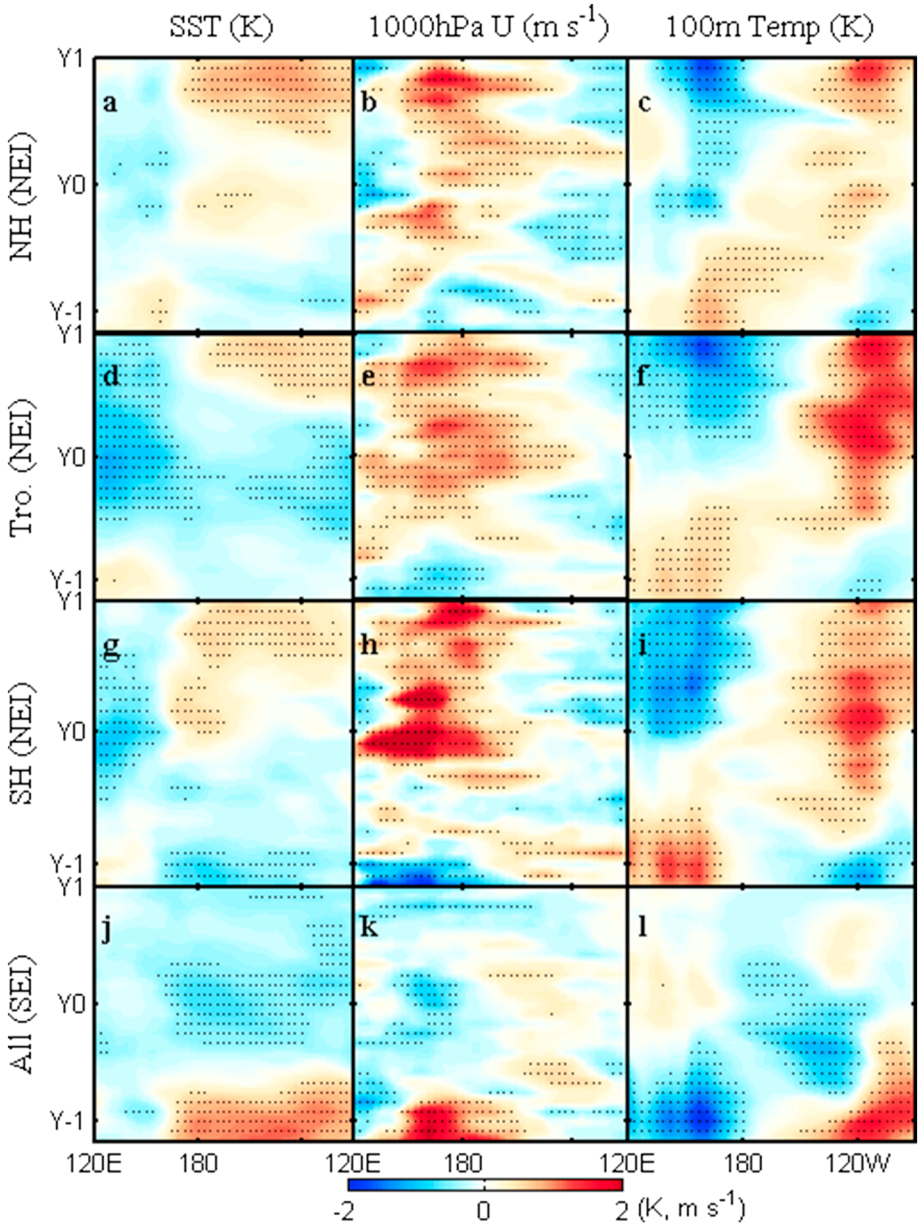

Figure 4. Simulated equatorial Pacific responses to different eruptions. Evolution of composite equatorial (10°S–10°N average; left panels) SST (K), (middle panels) 1,000-hPa zonal wind (m/s), and (right panels) 100-m oceanic temperature (K) anomalies for large (aerosol amount larger than 60 Tg) NH, tropical, and SH eruptions when the IOC is not a strong El Niño (NEI) and for all eruptions when the IOC is a strong El Niño (SEI; bottom panels). Stippling marks the anomalies significant above the 95% confidence level. Year −1 denotes the first winter (DJF) before the eruption, year 0 denotes the first winter after the eruption, and year 1 denotes the second winter.

2016), and the basin cooling also decays (Figure 4d); thus, the Bjerknes feedback acts to support the growth of El Niño.

In the first winter after SH eruptions for an NEI, strong westerly anomaly appears over the western equatorial Pacific (Figure 4h), mainly due to suppressed Australian monsoon and Southern Pacific Convergence Zone (not shown); then, the El Niño develops in the following year (Figures 4g–4i). When the IOC is already a strong El Niño, no El Niño-like signal can be found in both SST and thermocline in the first winter after any type of eruption (Figures 4j–4l), which means that the internal processes suppress the external forcing-induced responses.

4. Concluding Remarks

In this study, we investigate volcanic effects on ENSO in terms of both eruption type and IOC for the first time, using both reconstructions and CESM1 simulation. The strong El Niño-like IOC has a dominant impact on volcanic effects, and no significant El Niño-like warming is observed or simulated in the first and second winters after NH eruptions. Significant La Niña-like cooling, however, is also observed and simulated in the first winter following both tropical and SH eruptions. When the IOC does not involve a strong El Niño, eruption types determine volcanic effects. A significant El Niño-like response is observed in both reconstructions and model simulation in the second winter following NH eruptions. In the first winter following tropical eruptions, significant warming response is observed in the reconstructions. Meanwhile, a La Niña-like SST anomaly is simulated in the CESM1, even with an El Niño-like response in the thermocline for some cases, since the volcanic cooling is overestimated in CESM1. In both reconstructions and simulation, El Niño-like response is observed and simulated in the first winter after SH eruptions for an NEI, although this response is not stable because of small sample size. In both reconstructions and simulation, volcanic strength should be large enough to excite significant ENSO responses.

Based on the reconstruction analysis in this work, we have confidence to predict an El Niño in the second winter following NH eruptions and the first winter following tropical eruptions, except when the IOC shows a strong El Niño. The inconsistence of first-winter responses between reconstructions and simulation calls for further investigation and model improvement. Although our conclusions here are based on one model, it may still provide some guidance to the Model Intercomparison Project on the climate response to Volcanic forcing (Zanchettin et al., 2016). Such a project, however, can use more models to evaluate these volcanic effects.

Acknowledgments
This work was supported by the Natural Science Foundation of China (41420104002), the National Key Research and Development Program of China (2016YFA0600401), and by the Natural Science Foundation of Jiangsu (BK20150907, 14KJA170002). DC was supported by Swedish VR, VINOVVA, STINT, BECC, MERGE, and SNIC through S-CMIP. All reconstructions of three external forcing fields are available at http://pmip3.lsce.ipsl.fr/. The simulation results are available at https://pan.baidu.com/s/1eRJvzI6 (password: fpae). This paper is ESMC contribution 240.

References

Adams, J. B., Mann, M. E., & Ammann, C. M. (2003). Proxy evidence for an El Nino-like response to volcanic forcing. *Nature*, *426*(6964), 274–278. https://doi.org/10.1038/nature02101

Bellenger, H., Guilyardi, E., Leloup, J., Lengaigne, M., & Vialard, J. (2014). ENSO representation in climate models: From CMIP3 to CMIP5. *Climate Dynamics*, *42*(7–8), 1999–2018. https://doi.org/10.1007/s00382-013-1783-z

Braganza, K., Gergis, J. L., Power, S. B., Risbey, J. S., & Fowler, A. M. (2009). A multiproxy index of the El Niño–Southern Oscillation, A.D. 1525–1982. *Journal of Geophysical Research*, *114*, D05106. https://doi.org/10.1029/2008jd010896

Cai, W., Santoso, A., Wang, G., Yeh, S.-W., An, S.-I., Cobb, K. M., et al. (2015). ENSO and greenhouse warming. *Nature Climate Change*, *5*(9), 849–859. https://doi.org/10.1038/nclimate2743

Cook, E., D'Arrigo, R., & Anchukaitis, K. (2008). ENSO reconstructions from long tree-ring chronologies: Unifying the differences. Paper Presented at a Special Workshop on Reconciling ENSO Chronologies for the Past, Moorea, French Polynesia.

D'Arrigo, R., Cook, E. R., Wilson, R. J., Allan, R., & Mann, M. E. (2005). On the variability of ENSO over the past six centuries. *Geophysical Research Letters*, *32*, L03711. https://doi.org/10.1029/2004gl022055

D'Arrigo, R., Wilson, R., & Tudhope, A. (2009). The impact of volcanic forcing on tropical temperatures during the past four centuries. *Nature Geoscience*, *2*(1), 51–56. https://doi.org/10.1038/Ngeo393

Deser, C., Alexander, M. A., Xie, S. P., & Phillips, A. S. (2010). Sea surface temperature variability: Patterns and mechanisms. *Annual Review of Marine Science*, *2*(1), 115–143. https://doi.org/10.1146/annurev-marine-120408-151453.

Ding, Y. N., Carton, J. A., Chepurin, G. A., Stenchikov, G., Robock, A., Sentman, L. T., & Krasting, J. P. (2014). Ocean response to volcanic eruptions in Coupled Model Intercomparison Project 5 simulations. *Journal of Geophysical Research: Oceans*, *119*, 5622–5637. https://doi.org/10.1002/2013jc009780

Emile-Geay, J., Cobb, K. M., Mann, M. E., & Wittenberg, A. T. (2013). Estimating central equatorial Pacific SST variability over the past millennium. Part II: Reconstructions and implications. *Journal of Climate*, *26*(7), 2329–2352. https://doi.org/10.1175/Jcli-D-11-00511.1

Emile-Geay, J., Seager, R., Cane, M. A., Cook, E. R., & Haug, G. H. (2008). Volcanoes and ENSO over the past millennium. *Journal of Climate*, *21*(13), 3134–3148. https://doi.org/10.1175/2007jcli1884.1

Fischer, E. M., Luterbacher, J., Zorita, E., Tett, S. F. B., Casty, C., & Wanner, H. (2007). European climate response to tropical volcanic eruptions over the last half millennium. *Geophysical Research Letters*, *34*, L05707. https://doi.org/10.1029/2006gl027992

Gao, C., Robock, A., & Ammann, C. (2008). Volcanic forcing of climate over the past 1500 years: An improved ice core-based index for climate models. *Journal of Geophysical Research*, *113*, D23111. https://doi.org/10.1029/2008jd010239

Handler, P. (1984). Possible association of stratospheric aerosols and El Niño type events. *Geophysical Research Letters*, *11*(11), 1121–1124. https://doi.org/10.1029/GL011i011p01121

Haurwitz, M. W., & Brier, G. W. (1981). A critique of the superposed epoch analysis method: Its application to solar–weather relations. *Monthly Weather Review*, *109*(10), 2074–2079. https://doi.org/10.1175/1520-0493(1981)109<2074:acotse>2.0.co;2

Hegerl, G. C., Crowley, T. J., Baum, S. K., Kim, K.-Y., & Hyde, W. T. (2003). Detection of volcanic, solar and greenhouse gas signals in paleo-reconstructions of northern hemispheric temperature. *Geophysical Research Letters*, *30*(5), 1242. https://doi.org/10.1029/2002gl016635

Khodri, M., Izumo, T., Vialard, J., Janicot, S., Cassou, C., Lengaigne, M., et al. (2017). Tropical explosive volcanic eruptions can trigger El Niño by cooling tropical Africa. *Nature Communications*, *8*(1), 778. https://doi.org/10.1038/s41467-017-00755-6

Lehner, F., Schurer, A. P., Hegerl, G. C., Deser, C., & Frolicher, T. L. (2016). The importance of ENSO phase during volcanic eruptions for detection and attribution. *Geophysical Research Letters*, *43*, 2851–2858. https://doi.org/10.1002/2016gl067935

Li, J., Xie, S.-P., Cook, E. R., Huang, G., D'Arrigo, R., Liu, F., et al. (2011). Interdecadal modulation of El Niño amplitude during the past millennium. *Nature Climate Change*, *1*(2), 114–118. https://doi.org/10.1038/Nclimate1086

Li, J., Xie, S.-P., Cook, E. R., Morales, M. S., Christie, D. A., Johnson, N. C., et al. (2013). El Niño modulations over the past seven centuries. *Nature Climate Change*, *3*(9), 822–826. https://doi.org/10.1038/Nclimate1936

Lim, H. G., Yeh, S. W., Kug, J. S., Park, Y. G., Park, J. H., Park, R., & Song, C. K. (2016). Threshold of the volcanic forcing that leads the El Niño-like warming in the last millennium: Results from the ERIK simulation. *Climate Dynamics*, *46*(11–12), 3725–3736. https://doi.org/10.1007/s00382-015-2799-3

Liu, F., Chai, J., Wang, B., Liu, J., Zhang, X., & Wang, Z. (2016). Global monsoon precipitation responses to large volcanic eruptions. *Scientific Reports*, *6*(1), 24331. https://doi.org/10.1038/srep24331

Liu, F., Li, J., Wang, B., Liu, J., Li, T., Huang, G., & Wang, Z. (2018). Divergent El Niño responses to volcanic eruptions at different latitudes over the past millennium. *Climate Dynamics*, *50*(9-10), 3799–3812. https://doi.org/10.1007/s00382-017-3846-z

Maher, N., McGregor, S., England, M. H., & Sen Gupta, A. (2015). Effects of volcanism on tropical variability. *Geophysical Research Letters*, *42*, 6024–6033. https://doi.org/10.1002/2015gl064751

Mann, M. E., Cane, M. A., Zebiak, S. E., & Clement, A. (2005). Volcanic and solar forcing of the tropical Pacific over the past 1000 years. *Journal of Climate*, *18*(3), 447–456. https://doi.org/10.1175/Jcli-3276.1

Mann, M. E., Gille, E., Overpeck, J., Gross, W., Bradley, R. S., Keimig, F. T., & Hughes, M. K. (2000). Global temperature patterns in past centuries: An interactive presentation. *Earth Interactions*, *4*(4), 1–1. https://doi.org/10.1175/1087-3562(2000)004<0001:gtpipc>2.3.co;2

McGregor, S., & Timmermann, A. (2011). The effect of explosive tropical volcanism on ENSO. *Journal of Climate*, *24*(8), 2178–2191. https://doi.org/10.1175/2010jcli3990.1

McGregor, S., Timmermann, A., & Timm, O. (2010). A unified proxy for ENSO and PDO variability since 1650. *Climate of the Past*, *6*(1), 1–17. https://doi.org/10.5194/cp-6-1-2010

McPhaden, M. J., Zebiak, S. E., & Glantz, M. H. (2006). ENSO as an integrating concept in Earth science. *Science*, *314*(5806), 1740–1745. https://doi.org/10.1126/science.1132588

Myhre, G., Shindell, D., Bréon, F.-M., Collins, W., Fuglestvedt, J., Huang, J., et al. (2014). Anthropogenic and natural radiative forcing. In *Climate Change 2013: The Physical Science Basis. Contribution of Working Group I to the Fifth Assessment Report of the Intergovernmental Panel on Climate Change*, (pp. 659–740). Cambridge, UK, and New York: Cambridge Univ. Press. https://doi.org/10.1017/CBO9781107415324.018

Ohba, M., Shiogama, H., Yokohata, T., & Watanabe, M. (2013). Impact of strong tropical volcanic eruptions on ENSO simulated in a coupled GCM. *Journal of Climate*, *26*(14), 5169–5182. https://doi.org/10.1175/Jcli-D-12-00471.1

Pausata, F. S., Chafik, L., Caballero, R., & Battisti, D. S. (2015). Impacts of high-latitude volcanic eruptions on ENSO and AMOC. *Proceedings of the National Academy of Sciences of the United States of America*, *112*(45), 13,784–13,788. https://doi.org/10.1073/pnas.1509153112

Pausata, F. S., Karamperidou, C., Caballero, R., & Battisti, D. S. (2016). ENSO response to high-latitude volcanic eruptions in the northern hemisphere: The role of the initial conditions. *Geophysical Research Letters*, *43*, 8694–8702. https://doi.org/10.1002/2016gl069575

Predybaylo, E., Stenchikov, G. L., Wittenberg, A. T., & Zeng, F. (2017). Impacts of a Pinatubo-size volcanic eruption on ENSO. *Journal of Geophysical Research: Atmospheres*, *122*, 925–947. https://doi.org/10.1002/2016jd025796

Rayner, N. A., Parker, D. E., Horton, E., Folland, C. K., Alexander, L. V., Rowell, D. P., et al. (2003). Global analyses of sea surface temperature, sea ice, and night marine air temperature since the late nineteenth century. *Journal of Geophysical Research*, *108*(D14), 4407. https://doi.org/10.1029/2002JD002670

Robock, A. (2000). Volcanic eruptions and climate. *Reviews of Geophysics*, *38*(2), 191–219. https://doi.org/10.1029/1998rg000054

Robock, A., & Mao, J. (1992). Winter warming from large volcanic eruptions. *Geophysical Research Letters*, *19*(24), 2405–2408. https://doi.org/10.1029/92gl02627

Rosenbloom, N. A., Otto-Bliesner, B. L., Brady, E. C., & Lawrence, P. J. (2013). Simulating the mid-Pliocene warm period with the CCSM4 model. *Geoscientific Model Development*, *6*(2), 549–561. https://doi.org/10.5194/gmd-6-549-2013

Santer, B. D., Bonfils, C., Painter, J. F., Zelinka, M. D., Mears, C., Solomon, S., et al. (2014). Volcanic contribution to decadal changes in tropospheric temperature. *Nature Geoscience*, *7*(3), 185–189. https://doi.org/10.1038/Ngeo2098

Schurer, A. P., Tett, S. F. B., & Hegerl, G. C. (2014). Small influence of solar variability on climate over the past millennium. *Nature Geoscience*, *7*(2), 104–108. https://doi.org/10.1038/Ngeo2040

Sigl, M., Winstrup, M., McConnell, J. R., Welten, K. C., Plunkett, G., Ludlow, F., et al. (2015). Timing and climate forcing of volcanic eruptions for the past 2,500 years. *Nature*, *523*(7562), 543–549. https://doi.org/10.1038/nature14565

Stahle, D. W., Cleaveland, M. K., Therrell, M. D., Gay, D. A., D'Arrigo, R. D., Krusic, P. J., et al. (1998). Experimental dendroclimatic reconstruction of the southern oscillation. *Bulletin of the American Meteorological Society*, *79*(10), 2137–2152. https://doi.org/10.1175/1520-0477(1998)079<2137:edrots>2.0.co;2

Stevenson, S., Fasullo, J. T., Otto-Bliesner, B. L., Tomas, R. A., & Gao, C. (2017). Role of eruption season in reconciling model and proxy responses to tropical volcanism. *Proceedings of the National Academy of Sciences of the United States of America*, *114*(8), 1822–1826. https://doi.org/10.1073/pnas.1612505114

Stevenson, S., Otto-Bliesner, B., Fasullo, J., & Brady, E. (2016). "El Niño like" hydroclimate responses to last millennium volcanic eruptions. *Journal of Climate*, *29*(8), 2907–2921. https://doi.org/10.1175/jcli-d-15-0239.1

Wang, T., Guo, D., Gao, Y., Wang, H., Zheng, F., Zhu, Y., et al. (2017). Modulation of ENSO evolution by strong tropical volcanic eruptions. *Climate Dynamics* https://doi.org/10.1007/s00382-017-4021-2, *51*(7-8), 2433–2453.

Wilson, R., Cook, E., D'Arrigo, R., Riedwyl, N., Evans, M. N., Tudhope, A., & Allan, R. (2010). Reconstructing ENSO: The influence of method, proxy data, climate forcing and teleconnections. *Journal of Quaternary Science*, *25*(1), 62–78. https://doi.org/10.1002/jqs.1297

Yeh, S.-W., Cai, W., Min, S.-K., McPhaden, M. J., Dommenget, D., Dewitte, B., et al. (2018). ENSO atmospheric teleconnections and their response to greenhouse gas forcing. *Reviews of Geophysics*, *56*, 185–206. https://doi.org/10.1002/2017rg000568

Zanchettin, D., Khodri, M., Timmreck, C., Toohey, M., Schmidt, A., Gerber, E. P., et al. (2016). The Model Intercomparison Project on the climatic response to Volcanic forcing (VolMIP): Experimental design and forcing input data for CMIP6. *Geoscientific Model Development*, *9*(8), 2701–2719. https://doi.org/10.5194/gmd-9-2701-2016